Multimodality imaging to distinguish between benign and malignant cardiac masses

Ayaz Aghayev, MD,[a] Michael K. Cheezum, MD,[b] Michael L. Steigner, MD,[a] Negareh Mousavi, MD,[c] Robert Padera, MD,[d] Ana Barac, MD, PhD,[e] Raymond Y. Kwong, MD,[f] Marcelo F. Di Carli, MD,[g] and Ron Blankstein, MD, FACC[g]

[a] Cardiovascular Imaging Program, Department of Radiology, Brigham and Women's Hospital, Harvard Medical School, Boston, MA
[b] Department of Cardiology, Parkview Health, Fort Wayne, IN
[c] Cardiovascular Division, McGill University Health Center, Montreal, QC, Canada
[d] Department of Pathology, Brigham and Women's Hospital, Boston, MA
[e] MedStar Heart and Vascular Institute, Georgetown University, Washington, DC
[f] Cardiovascular Imaging Program, Cardiovascular Division, Brigham and Women's Hospital, Harvard Medical School, Boston, MA
[g] Cardiovascular Imaging Program, Cardiovascular Division and Department of Radiology, Brigham and Women's Hospital, Harvard Medical School, Boston, MA

Received May 25, 2021; accepted Jul 25, 2021
doi:10.1007/s12350-021-02790-9

Background. **To compare the diagnostic accuracy of CMR and FDG-PET/CT and their complementary role to distinguish benign vs malignant cardiac masses.**

Methods. **Retrospectively assessed patients with cardiac mass who underwent CMR and FDG-PET/CT within a month between 2003 and 2018.**

Results. **72 patients who had CMR and FDG-PET/CT were included. 25 patients (35%) were diagnosed with benign and 47 (65%) were diagnosed with malignant masses. 56 patients had histological correlation: 9 benign and 47 malignant masses. CMR and FDG-PET/CT had a high accuracy in differentiating benign vs malignant masses, with the presence of CMR features demonstrating a higher sensitivity (98%), while FDG uptake with SUVmax/blood pool ≥ 3.0 demonstrating a high specificity (88%). Combining multiple (> 4) CMR features and FDG uptake (SUVmax/blood pool ratio ≥ 3.0) yielded a sensitivity of 85% and specificity of 88% to diagnose malignant masses. Over a mean follow-up of 2.6 years (IQR 0.3-3.8 years), risk-adjusted mortality were highest among patients with an infiltrative border on CMR (adjusted HR 3.1; 95% CI 1.5-6.5; $P = .002$) or focal extracardiac FDG uptake (adjusted HR 3.8; 95% CI 1.9-7.7; $P < .001$).**

Conclusion. **Although CMR and FDG-PET/CT can independently diagnose benign and malignant masses, the combination of these modalities provides complementary value in select cases. (J Nucl Cardiol 2022;29:1504–17.)**

Supplementary Information The online version contains supplementary material available at https://doi.org/10.1007/s12350-021-02790-9.

Funding None.

The authors of this article have provided a PowerPoint file, available for download at SpringerLink, which summarizes the contents of the paper and is free for re-use at meetings and presentations. Search for the article DOI on SpringerLink.com.

JNC thanks Erick Alexanderson MD, for providing the Spanish abstract and Weihua Zhou, Ph.D. for providing the Chinese abstract.

Reprint requests: Ayaz Aghayev, MD, Cardiovascular Imaging Program, Department of Radiology, Brigham and Women's Hospital, Harvard Medical School, Boston, MA, USA; *aaghayev@bwh.harvard.edu*

1071-3581/$34.00

Chinese Abstract

背景. 本研究旨在比较心脏磁共振 **(CMR)** 和FDG-PET/CT的诊断准确性及其在鉴别心脏良恶性肿瘤中的互补作用。

方法. 本研究回顾性地纳入了2003-2018年间在本中心被诊断为心脏肿瘤的患者，所有患者CMR和FDG-PET/CT检查均在一个月内完成。

结果. 本研究纳入了72例同时接受了CMR和FDG-PET/CT检查的患者。其中25例（35%）患者被诊断为心脏良性肿瘤，47例（65%）患者被诊断为心脏恶性肿瘤。在所有72例患者中，56例（9例良性和47例恶性）有组织学诊断的证据。CMR和FDG-PET/CT在鉴别心脏良性和恶性肿瘤方面具有较高的准确性。其中CMR的特点表现为较高的敏感性（98%），而当FDG摄取为SUVmax/血池≥ 3.0时，FDG-PET/CT有较高的特异性（88%）。结合多种CMR特征（> 4种）和FDG摄取程度（SUVmax/血池比率≥ 3.0）用于心脏恶性肿瘤的诊断时，其敏感性为85%，特异性为88%。平均随访2.6年后（IQR:0.3-3.8年），CMR表现为边界浸润（调整后HR=3.1；95%可信区间：1.5-6.5；p=0.002）或局灶性心脏外FDG摄取（校正HR=3.8；95%可信区间：1.9-7.7；p<0.001）的患者，风险校正后的死亡率最高。

结论. 尽管CMR和FDG-PET/CT可以独立地用于诊断心脏良性和恶性肿瘤，但在某些特定病例中，将这两种方法结合具有互补的诊断价值。 **(J Nucl Cardiol 2022;29:1504–17.)**

Spanish Abstract

Antecedentes. **Comparar la precisión diagnóstica de la RMC y del PET/CT con FDG y su función complementaria para distinguir entre masas cardíacas benignas y malignas.**

Métodos. **Pacientes evaluados retrospectivamente con masas cardíacasque se sometieron a RMC y a PET/CT con FDG en un periodo de 1 mes entre 2003-2018.**

Resultados. **Se incluyeron 72 pacientes a los que se les realizó RMC y PET/CT con FDG. 25 pacientes (35%) fueron diagnosticados como masas benignas y 47 (65%) como masas malignas. 56 pacientes tuvieron correlación histológica: 9 masas benignas y 47 malignas.La RMC y el PET/CT con FDG tuvieron una alta precisión en la diferenciación de masas benignas de malignas, algunas caracteristicas de la RMC demostraron una mayor sensibilidad (98 %), mientras que una captación de FDG (SUVmax/poolsanguíneo ≥ 3.0)demostró una alta especificidad (88%). Combinando múltiples (>4) características de la RMC con la captación de FDG (SUVmax/poolsanguíneo ≥ 3,0)se obtuvo una sensibilidad del 85% y una especificidad del 88 % para diagnosticar masas malignas. Durante un seguimiento promedio de 2.6 años (ICR: 0.3-3.8 años), la mortalidad ajustada por riesgo fue más alta entre los pacientes con un borde infiltrante en la RMC (HR ajustado = 3.1; IC del 95 %: 1.5-6.5;p=0.002) o captación extracardiaca focal de FDG (HR ajustado=3.8; IC 95%: 1.9-7.7; p<0.001).**

Conclusión. **Aunque la RMC y e lPET/CT con FDG pueden diagnosticar de forma independiente masas benignas y malignas, la combinación de estas modalidades proporciona un valor complementario en casos seleccionados. (J Nucl Cardiol 2022;29:1504–17.)**

Key Words: MRI · PET · modalities

Abbreviations

CMR	Cardiac magnetic resonance imaging
FDG-PET/CT	Fluorodeoxyglucose-Positron Emission Tomography/Computed Tomography
DIR	Double inversion recovery
LGE	Late gadolinium enhancement
FPP	First pass perfusion
SUV	Standardized uptake value
AUC	Area under the curve
LHIS	Lipomatous hypertrophy of interatrial septum

See related editorial, pp. 1518–1519

INTRODUCTION

Cardiac masses are rare entities associated with significant morbidity and mortality.[1,2] They can be classified as non-neoplastic, benign neoplastic, primary malignant, or secondary malignant (metastatic) masses. Non-neoplastic masses particularly thrombus, pericardial cysts, and lipomatous hypertrophy of the septum that mimic tumors[3] are the most common masses. Primary cardiac neoplasms are rare, with an estimated prevalence of 0.001% to 0.03% in autopsy series,[4] while secondary malignant/metastases masses are 20 to 40 times more common than primary cardiac neoplasms.[4,5]

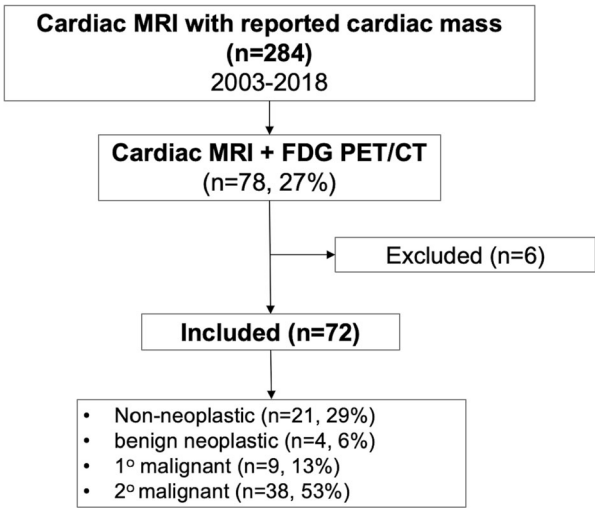

Figure 1. Patient flow chart.

Cardiac imaging plays a vital role in the diagnosis and management of cardiac masses, partly due to the challenges of performing direct biopsy. Echocardiography is a widely available and is usually the first-line imaging test. Cardiac computed tomography (CT) is increasingly utilized to evaluate cardiac masses in certain scenarios.[6] However, cardiac magnetic resonance (CMR) imaging is preferred because it can integrate the assessment of cardiac structures and function, as well as tissue characterization.[7,8] Although CMR has a high accuracy to identify benign lesions, the diagnosis of malignant cases can be challenging.[2] However, metabolic information using fluorodeoxyglucose-positron emission tomography (FDG-PET) can provide further diagnostic information when there is a suspicion for malignant masses.[9–11] Nevertheless, there are limited data regarding the complementary role of CMR and FDG-PET/CT in the evaluation of cardiac masses. In addition, there are no established guidelines on how to integrate the information from these techniques in the evaluation of patients with cardiac masses.

Our objective was to evaluate the complementary value of CMR and FDG-PET/CT to distinguish between benign and malignant cardiac masses and to describe the prognostic value of these techniques to inform risk assessment.

MATERIALS AND METHODS

Study Population

Institutional review board approval was obtained and due to the retrospective nature of the study, the requirement for written informed consent was waived. Using an electronic search of CMR imaging database at Brigham and Women's Hospital (Boston, MA), we retrospectively identified 284 patients with reported cardiac mass on imaging between 2003 and 2018. Of these, 78 patients underwent FDG-PET/CT to assess local metabolic activity or disease staging within a month of the CMR study. Patients with FDG-PET/CT performed after cardiac mass resection (N = 1) were excluded as those who were treated with chemotherapy between imaging studies (N = 2), those with FDG-PET/CT studies performed >1 month before or after the CMR (N = 2), and those with inconclusive diagnosis (N = 1). Consequently, 72 patients who had CMR and FDG-PET/CT imaging studies within a month of each other were included in the study (Figure 1). A total of 38 patients in this study were included in our previous work, where we assessed cardiac masses by CMR only.[2]

Individual patient electronic medical records were retrospectively reviewed to obtain demographics, clinical data, other cardiac imaging findings (e.g., transthoracic echocardiography [TTE], transesophageal echocardiography [TEE], CT), source of tissue sampling, cardiac and/or extracardiac histopathology results, treatment, and clinical status at last follow-up.

Cardiac MRI

CMR studies were performed on a 1.5-T scanner (Magnetom Avanto eco, Siemens) with an 8- or 12-element cardiac phased-array coil or a 3.0-T scanner (Magnetom TIM TRIO, Siemens) with a 16-element phased-array coil and electrocardiographic gating. In all cases, a standard cardiac mass protocol was used, including image sequences to evaluate morphological, functional, and tissue characterization of the mass.

High-resolution cine images were obtained using steady-state free precession sequences in multiple planes. Pre- and postcontrast images were obtained using double inversion recovery (DIR) fast spin-echo T1-weighted (T1W) and T2-weighted (T2W) sequences with and without fat suppression. Intravenous gadolinium diethylenetriamine pentaacetic acid (DTPA) chelate was administered at a dose appropriate for patient weight (0.1-0.2 mmol□kg) with postcontrast imaging for first-pass perfusion (FPP) and late gadolinium enhancement (LGE) of the cardiac mass. Phase-sensitive inversion recovery sequences were used in conjunction with all LGE images. CMR examinations were obtained in conventional and complementary cardiac planes suited to evaluate the cardiac mass, and a physician experienced in cardiac imaging was present for the acquisition of all studies.

FDG-PET/CT Imaging

FDG-PET imaging was performed from the base of the skull through the proximal thigh using Discovery LS, Discovery DSTE/VCT64, and Discovery DRX/VCT64 scanners (GE Medical Systems, Waukesha, WI). Patients were instructed to fast for a minimum of 4 to 6 hours prior to the study and had a mean blood glucose level of 99 ± 16 mg□dL. There was no dedicated diet for myocardial suppression.

Approximately 60 minutes following administration of FDG (mean dose: 543 ± 55 MBq) via a peripheral vein, image acquisition was obtained with no electrocardiogram (ECG) gating as a part of the institutional protocol for cancer imaging. Non-contrast, low-dose helical CT imaging (120-140 kV; 80 mA) was performed over the same range without breath-hold for attenuation correction of PET images and anatomic correlation.

Blinded Image Analysis

CMR and FDG-PET/CT images were retrospectively reviewed for all patients by an advanced cardiovascular imaging and PET/CT (onco-radiology) fellowship-trained radiologist (A.A.) blinded to all clinical data, histopathology results, and outcomes. CMR exams were analyzed using a dedicated CMR workstation (Medis Medical Imaging Systems BV, QMass MR 7.4, Leiden, the Netherlands) to describe the following mass features: (1) size (cm); (2) location (intracavitary, valvular, intramyocardial, interatrial septum, pericardial, extrapericardial with cardiac extension); (3) signal intensity on DIR fast spin-echo T1W and T2W images (isointense, hypointense, or hyperintense relative to normal myocardium); (4) fat suppression (yes/no); (5) pericardial effusion (present if effusion diameter >10 mm at end diastole); (6) FPP (present/absent); (7) LGE (present/absent); (8) mobility (yes/no); and (9) mass shape to determine if it was a "well-defined" or an "infiltrative pattern." It was considered an "infiltrative pattern" if the lesion had an irregular shape with poorly defined margins and appeared to invade adjacent tissues.

FDG-PET images were analyzed blinded to CMR and clinical data using a dedicated nuclear imaging workstation, Hermes Gold (Hermes Medical Solutions, AB, Stockholm, Sweden). Attenuation-corrected FDG-PET images were used to obtain the maximum standardized uptake value (SUV_{max}) in a region of interest containing the mass. In the absence of focal FDG uptake, SUV_{max} was taken from a region of interest at the location of the suspected mass. In addition, SUV_{max} values of extracardiac FDG uptake were collected if present. A 1-cm region of interest was drawn in the superior vena cava at the level of the main pulmonary artery to obtain the mean blood pool standard uptake value (SUV) and used to calculate the lesion SUV_{max}/-blood pool ratio.

Outcome and Clinical Diagnosis Assessment

Death from any cause was obtained using the Social Security Death Index and electronic medical records in the Research Patient Data Registry. This centralized clinical data registry contains data from all institutions in the Mass General Brigham system.

Death analysis was stratified by histology diagnosis obtained from pathology specimen (N = 56/72, 78%) obtained from a cardiac (N = 27, 48%) or extracardiac source (N = 29, 52%). A final clinical diagnosis in all patients was determined by incorporating CMR and FDG-PET/CT findings, histopathology when available (N = 56, 78%), and a history of known malignancy (N = 45, 63%). Histopathology and final clinical diagnosis were determined at the time of initial staging following CMR and FDG-PET/CT.

Statistical Analysis

Continuous data with normal distributions are presented as mean ± SD and compared with the Student's *t* test for 2 independent groups and 1-way analysis of variance for multiple groups. Continuous variables with non-normal distributions are presented as median with interquartile range (IQR) 25th to 75th percentile and compared with the Wilcoxon rank-sum test. Categorical variables are presented as frequencies (%) and compared using the Pearson χ^2 test or Fisher exact test for small group comparisons (observed frequency $N < 5$ in any subgroup). Receiver operating characteristic (ROC) analysis was performed to determine the area under the curve (AUC) of CMR and FDG-PET/CT features to discriminate between a benign and a malignant mass. Additionally, ROC analysis was used to determine the optimal cut-off of lesion SUV_{max}/blood pool ratio and mass diameter. Cut-points for each variable were determined by their optimal trade-off between sensitivity and specificity to discriminate between a benign and a malignant mass.

To describe the event-free survival of patients with a malignant vs a benign cardiac mass, we constructed Kaplan–Meier curves with survival comparison by log-rank analysis according to the elapsed time since the CMR. Cox proportional hazard ratios were estimated for all-cause mortality. All analyses were performed using

Table 1. Patient characteristics stratified by cardiac mass type

	All patients (N = 72)	Benign (N = 25)	Malignant (N = 47)	*P* value
Age, years, median [IQR][a]	63 [49,68]	65 [42,69]	62 [51,67]	.97
Male, N (%)	38 (53%)	16 (64%)	22 (47%)	.16
History of prior malignancy before CMR and FDG-PET, N (%)	45 (63%)	14 (56%)	31 (66%)	.68
Time between CMR and FDG-PET, days, median [IQR][b]	1 [−5,14]	−2 [−14,8]	4 [−2,14]	.09
Death in follow-up, N (%)	39 (54%)	10 (40%)	29 (62%)	.08
Time to clinical follow-up or death, years, mean [IQR]	2.6 [0.3,3.8]	3.9 [0.8,7.2]	1.9 [0.3,2.1]	.02
Cardiac symptoms, N (%)				
None	34 (47%)	13 (52%)	21 (45%)	.57
Dyspnea	11 (15%)	2 (8%)	9 (19%)	
Chest pain	12 (17%)	3 (12%)	9 (19%)	
Palpitations/arrhythmia	5 (7%)	2 (8%)	3 (6%)	
Presyncope/syncope	1 (1%)	0 (0%)	1 (2%)	
Edema/CHF	2 (3%)	1 (4%)	1 (2%)	
TIA/CVA	4 (6%)	3 (12%)	1 (2%)	
Other	3 (4%)	1 (4%)	2 (4%)	

Values expressed as N (%), mean ± SD or median [IQR].
[a]Patient age at the time of initial CMR or FDG-PET exam.
[b]Thirty-nine (54%) patients had CMR first, 27 (38%) had FDG-PET first, and 6 (8%) patients had same day CMR and FDG-PET.

Stata (v13.1, Statacorp) and a 2-tailed $P < .05$ was considered significant.

RESULTS

Patient characteristics are presented in Table 1, stratified by malignant or benign cardiac masses. The median age at the time of initial imaging was 63 years (IQR 49-68) and there was a similar proportion of males vs. females. A majority of patients had a history of prior malignancy (N = 45, 63%).

The final clinical diagnoses for all patients are categorized in Table 2 as non-neoplastic (29%), benign neoplastic (6%), primary malignant (13%), or secondary malignant/metastatic masses (53%). Direct histopathology was available for 56 (78%) patients, including 9 benign and 47 malignant masses. In 16 patients (22%) no biopsy was performed because of a characteristic imaging finding of thrombus (N = 7), lipomatous hypertrophy of the interatrial septum (LHIS; N = 6), mitral annular calcification (N = 1), thrombosed left circumflex coronary artery aneurysm (N = 1), and pericardial cyst (N = 1).

CMR Imaging Characteristics

Table 3 demonstrates individual CMR features stratified by mass type. Compared with benign masses, malignant lesions were larger, more often intramyocardial, pericardial, or extrapericardial with cardiac extension and more often right-sided when intracavitary. Malignant masses were typically T1W isointense and T2W hyperintense relative to myocardium malignant masses which were also more likely to demonstrate first-pass perfusion, to have an infiltrative appearance and to demonstrate evidence of LGE within the mass.

Figure 2 demonstrates the frequency of CMR features stratified by benign and malignant mass type. By ROC analysis, a CMR-derived maximum mass diameter ≥ 4.3 cm provided the greatest combination of sensitivity (Sn = 62%) and specificity (Sp = 88%) to discriminate benign from malignant lesions with ROC AUC = 0.75 (95% CI 0.69-0.90).

Table 2. Cardiac mass clinical and histology diagnosis following CMR and ^{18}F-FDG-PET-CT

		Final diagnosis with histology (N = 56)	
	Final diagnosis all patients (N = 72)	**Benign (N = 9)**	**Malignant (N = 47)**
Benign, N (%)	25 (35%)	9 (100%)	-
Non-neoplastic	21 (29%)	5 (56%)	-
Cardiac thrombus	10 (14%)	3 (33%)	-
Fibroadipose tissue	1 (1%)	1 (11%)	-
Left atrium intracavitary calcified amorphous tumor (CAT)	1 (1%)	1 (11%)	-
Lipomatous hypertrophy	6 (8%)	0	-
Mitral annular calcification	1 (1%)	0	-
Thrombosed LCX aneurysm	1 (1%)	0	-
Pericardial cyst	1 (1%)	0	-
Benign neoplastic	4 (6%)	4 (44%)	-
Paraganglioma	3 (4%)	3 (33%)	-
Myxoma	1 (1%)	1 (11%)	-
Malignant	47 (65%)	-	47 (100%)
Primary malignant	9 (13%)	-	9 (19%)
Spindle cell sarcoma	4 (6%)	-	4 (9%)
Paraganglioma	2 (3%)	-	2 (4%)
Angiosarcoma	1 (1%)	-	1 (2%)
Undifferentiated sarcoma	1 (1%)	-	1 (2%)
Synovial cell sarcoma	1 (1%)	-	1 (2%)
Secondary malignant (Metastatic)	38 (53%)		38 (81%)
Melanoma	5 (7%)	-	5 (11%)
Lymphoma	5 (7%)	-	5(11%)
Mesothelioma	5 (7%)	-	5 (11%)
Lung carcinoma, undifferentiated	5 (7%)	-	5 (11%)
Leukemia	3 (4%)	-	3 (6%)
Squamous cell carcinoma (mouth)	3 (4%)	-	3 (6%)
Inflammatory histiocytic neoplasm (Erdheim–Chester disease)	2 (3%)	-	2 (4%)
Renal cell carcinoma	2 (3%)	-	2 (4%)
Squamous cell carcinoma (thymus)	1 (1%)	-	1 (2%)
Squamous cell/NSCLC (lung)	1 (1%)	-	1 (2%)
Angiosarcoma (breast)	1 (1%)	-	1 (2%)
Leiomyosarcoma	1 (1%)	-	1 (2%)
Merkel cell carcinoma	1 (1%)	-	1 (2%)
Cholangiocarcinoma	1 (1%)	-	1 (2%)
Breast carcinoma	1 (1%)	-	1 (2%)
Indeterminate, likely colon cancer	1 (1%)	-	1 (2%)

CMR, cardiac magnetic resonance imaging; *LCX*, left circumflex coronary artery; *NSCLC*, non-small cell lung carcinoma; *FDG-PET/CT*, fluorodeoxyglucose-positron emission tomography/computed tomography. Values are N (%).

FDG-PET/CT Imaging Characteristics

FDG-PET/CT imaging characteristics for all patients are detailed in Table 4. Overall, 51 patients had focal FDG uptake (greater than blood pool) of the cardiac mass with an SUVmax of 9.6 [6.3,14.1]; the majority of such masses were malignant tumors (N = 45, 96%). A total of 6 benign masses, including 2 lipomatous hypertrophy of the interatrial septum (LHIS), 3

Table 3. CMR characteristics stratified by cardiac mass type

	All patients (N = 72)	Benign (N = 25)	Malignant (N = 47)	*P* value
Left ventricular ejection fraction, %	59 [55,63]	60 [50,65]	59 [55,63]	.82
Maximum mass diameter, cm	4.0 [2.6,6.2]	2.6 [1.7,4.1]	4.7 [3.2,6.7]	< .001
Mass location, N (%)				
Intracavitary, N (%)	16 (22%)	11 (44%)	5 (11%)	< .001
[# right heart/# left heart]	[11/5]	[6/5]	[5/0]	
Valvular	1 (1%)	1 (4%)	0 (0%)	
Intramyocardial	19 (26%)	2 (8%)	17 (36%)	
Interatrial septum	7 (10%)	6 (24%)	1 (2%)	
Pericardial	21 (29%)	5 (20%)	16 (34%)	
Extrapericardial with cardiac extension	8 (11%)	0 (0%)	8 (17%)	
T1W characteristics				
Isointense	47 (65%)	8 (32%)	39 (83%)	<.001
Hypointense	7 (10%)	6 (24%)	1 (2%)	
Hyperintense	12 (17%)	9 (36%)	3 (6%)	
Heterogeneous intensity	6 (8%)	2 (8%)	4 (9%)	
T2W characteristics				
Isointense	3 (4%)	3 (12%)	0 (0%)	< .001
Hypointense	5 (7%)	5 (20%)	0 (0%)	
Hyperintense	55 (76%)	15 (60%)	40 (85%)	
Heterogeneous intensity	9 (13%)	2 (8%)	7 (15%)	
Not fat suppressed	65 (90%)	19 (76%)	46 (98%)	.001
Pericardial effusion	18 (25%)	2 (8%)	16 (34%)	.01
First pass perfusion[a]	39 (60%)	5 (20%)	34 (83%)	< .001
LGE (in mass)	51 (71%)	6 (24%)	45 (96%)	<.001
Nonmobile	65 (90%)	20 (80%)	45 (96%)	.045
Mass shape				
Well-defined border	29 (40%)	22 (88%)	7 (15%)	<.001
Infiltrative appearance	43 (60%)	3 (12%)	40 (85%)	

Values expressed as N (%), mean ± SD or median [IQR]
CMR, cardiac magnetic resonance imaging; *LGE*, late gadolinium enhancement.
[a]Seven patients (1 benign, 6 malignant) did not have first pass perfusion imaging.

paragangliomas, and 1 fibroadipose mass, had focal FDG uptake. An optimal SUV_{max}/blood pool ratio cut-off ≥ 3.0 provided the best trade-off between sensitivity (Sn = 85%) and specificity (Sp = 88%) to detect malignancy (AUC = 0.88; 95% CI 0.77-0.98; Supplementary figure 1), correctly classifying 86% of patients with a positive likelihood ratio (+ LR) = 7.10 and negative likelihood ratio (− LR) = 0.17. Twenty-four of the 45 patients with malignant lesions (53%) had extracardiac FDG uptake from metastatic disease of their primary extracardiac malignancy. Six patients with benign cardiac masses (4 LHIS, 2 thrombus) had focal extracardiac FDG uptake related to know malignancy and only 1 of these patients had FDG uptake associated with the benign cardiac mass (N = 1, LHIS). The mean SUVmax value of the remote and normal myocardium in all patients measured 2.2 [1.5, 2.9].

Combined CMR and FDG-PET/CT Findings

Among 47 malignant masses, 46 (98%) had more than 4 (out of 9) CMR features of malignancy, with a median SUVmax of 9.6 (IQR 6.5, 13.7). Outliers provide important case examples regarding the limitations of CMR and FDG-PET/CT to provide a final diagnosis and are summarized here. One patient had malignant laminated squamous cells on histopathology with extensive necrosis and associated thrombus, with only 2 CMR features of malignancy (T1 isointense and not fat suppressed) and a cardiac SUV/blood pool ratio =

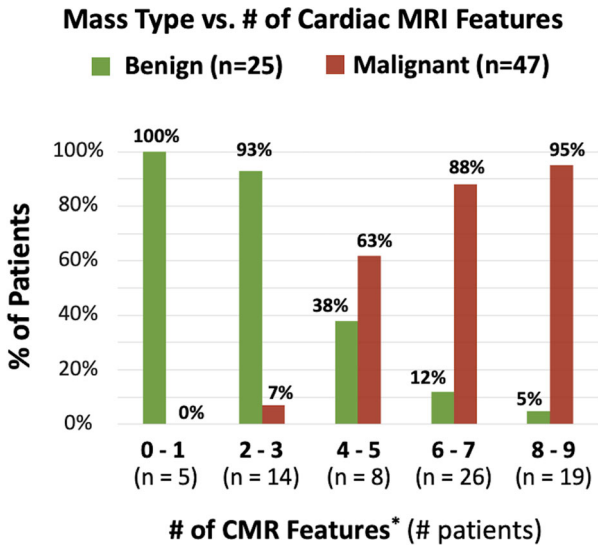

Figure 2. Mass type stratified by number of cardiac magnetic resonance (CMR) features. Nine CMR features included T1 isointense, T2 hyperintense, pericardial effusion, first-pass perfusion, late gadolinium enhancement (LGE), not fat suppressed, intramyocardial or pericardial, mass diam. ≥ 4.3 cm, and infiltrative appearance.

0.9 (SUV_{max} of 1.9). One patient with a history of prostate cancer had a benign fibroadipose cardiac mass, had 8 out of 9 CMR features of malignancy, and a mild cardiac uptake with an SUV/blood pool ratio = 1.8 (SUV_{max} of 4.7) (Figure 3A). Two patients with a benign paraganglioma had significantly elevated SUV/blood pool ratios, with ≥6 CMR features of malignancy (Figure 3B).

The diagnostic performance of CMR and FDG-PET/CT features is detailed in Figure 4 and supplementary Table 1. Both CMR (> 4 imaging features) and FDG-PET/CT (SUV_{max}/blood pool ratio cut-off ≥ 3.0 or $SUV_{max} > 5.9$) had a high AUC to diagnose malignancy. However, combining these two modalities (CMR more than 4 imaging features and FDG-PET/CT [SUV_{max}/-blood pool ratio cut-off ≥ 3.0]) did not increase the diagnostic accuracy for malignant masses (AUC 0.87; 95% CI 0.78-0.95) (Figure 5).

Outcomes

The mean duration of follow-up after the diagnosis was 2.6 years (IQR 0.3-3.8) and 39 (54%) of 72 patients

Table 4. FDG-PET characteristics stratified by cardiac mass type

	All patients (N = 72)	Benign (N = 25)	Malignant (N = 47)	*P* value
Cardiac mass uptake				
FDG uptake in the mass, N (%)	51 (71%)	6 (24%)	45 (96%)	< 0.001
Cardiac SUV_{max} (all patients)[a]	7.3 [2.1,11.0]	1.8 [1.7,2.3]	9.6 [6.5,13.7]	<0.001
Cardiac SUV_{max} (focal uptake)	9.6 [6.3,14.1]	5.6 [5.2,24.1]	9.6 [7.3,13.7]	0.40
Extracardiac uptake				
Extracardiac FDG uptake	29 (40%)	5 (20%)	24 (51%)	0.01
Extracardiac SUV_{max}	11.2 [7.5,17.5]	7.1 [5.6,7.5]	12.9 [9.7,17.9]	0.02
Background uptake				
Blood pool SUV_{mean}[b]	1.8 [1.5,2.0]	1.8 [1.6,2.0]	1.9 [1.4,2.1]	0.90
Liver SUV_{mean}[c]	2.6 [2.3,3.3]	2.7 [2.3,3.2]	2.6 [2.2,3.3]	0.98
Cardiac mass/background (all patients)				
Cardiac SUV_{max}/blood pool ratio	3.9 [1.2,6.6]	1.1 [0.9,1.3]	5.6 [3.5,8.4]	< 0.001
Cardiac SUV_{max}/liver ratio	2.6 [0.8,4.2]	0.7 [0.6,1.0]	3.8 [2.6,4.6]	< 0.001
Cardiac mass/background (focal mass uptake only)				
Cardiac SUV_{max}/blood pool ratio	5.6 [3.5,8.6]	3.9 [2.4,11.0]	5.7 [3.8,8.4]	0.40
Cardiac SUV_{max}/liver ratio	3.8 [2.6,4.8]	2.4 [1.9,6.7]	3.8 [2.6,4.6]	0.47

Values expressed as N (%), mean ± SD or median [IQR].
Blood pool SUV_{mean} taken from a 1-cm region of interest in superior vena cava at the level of pulmonary artery bifurcation.
FDG-PET, ^{18}F-labeled fluorodeoxyglucose-positron emission tomography, *SUV*, standardized uptake value.
[a]Seven patients (1 benign, 6 malignant) did not have first-pass perfusion imaging.
In patients with no FDG uptake in the mass, cardiac SUV_{max} was taken from the region of interest at the location of the suspected mass.
[b]Seven patients (1 benign, 6 malignant) did not have first-pass perfusion imaging.

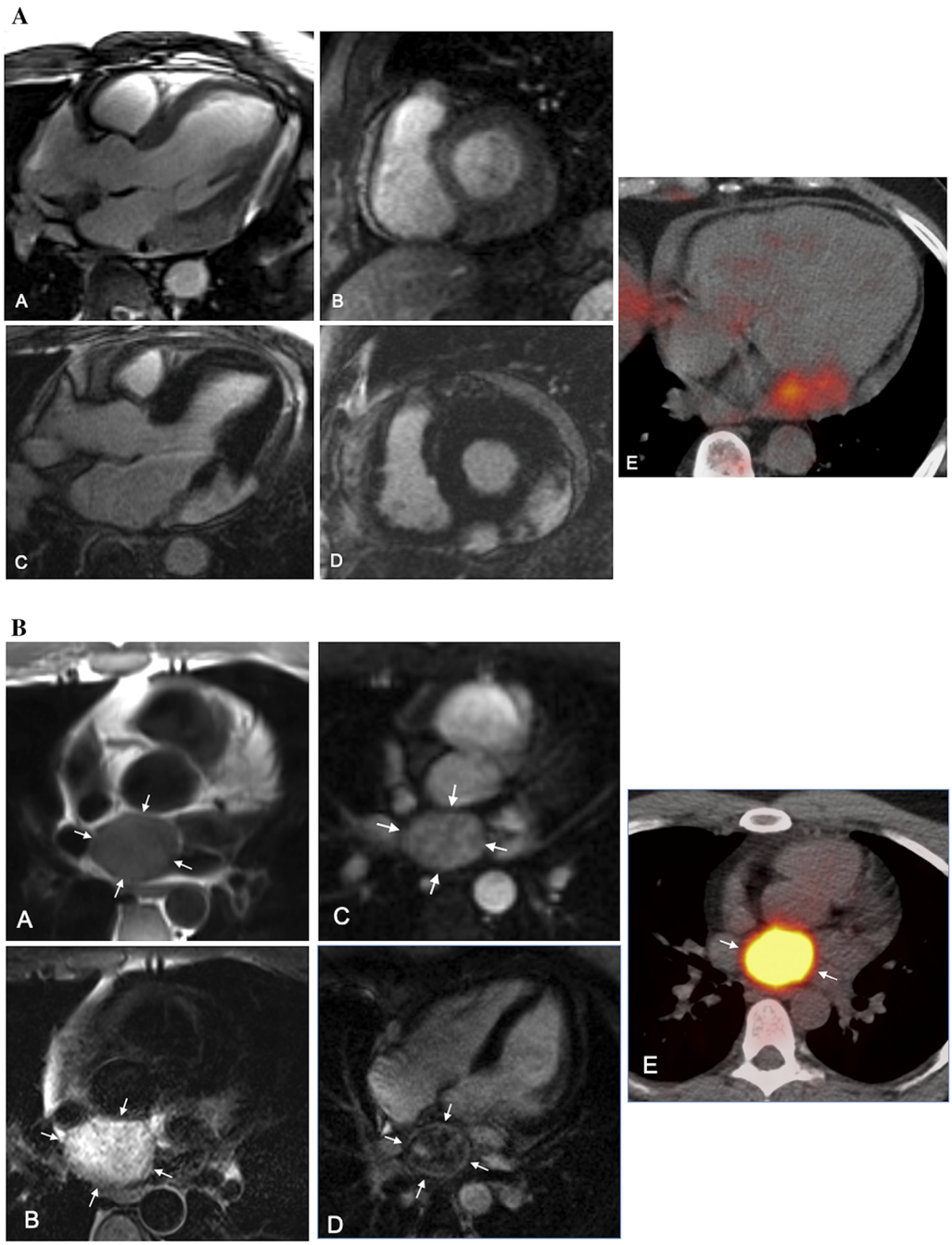

Figure 3. A Pathology-proven fibroadipose tissue in a patient with a history of prostate cancer demonstrates hyperintense signal intensity on (A) free precession steady-state cine image. The mass has avid enhancement on (B) first-pass perfusion and significant amount of gadolinium retention on (C, D) late gadolinium enhancement 3 chamber and short-axis images. (E) FDG-PET/CT image shows mild FDG uptake in the mass (SUVmax of 4.7). **B** Pathology-proven benign paraganglioma demonstrates isointense signal intensity on (A) T1-weighted hyperintense and on (B) T2-weighted images. The mass has avid enhancement on (C) first-pass perfusion and gadolinium retention on (D) late gadolinium enhancement. (E) FDG-PET/CT image through the mass shows intense FDG uptake.

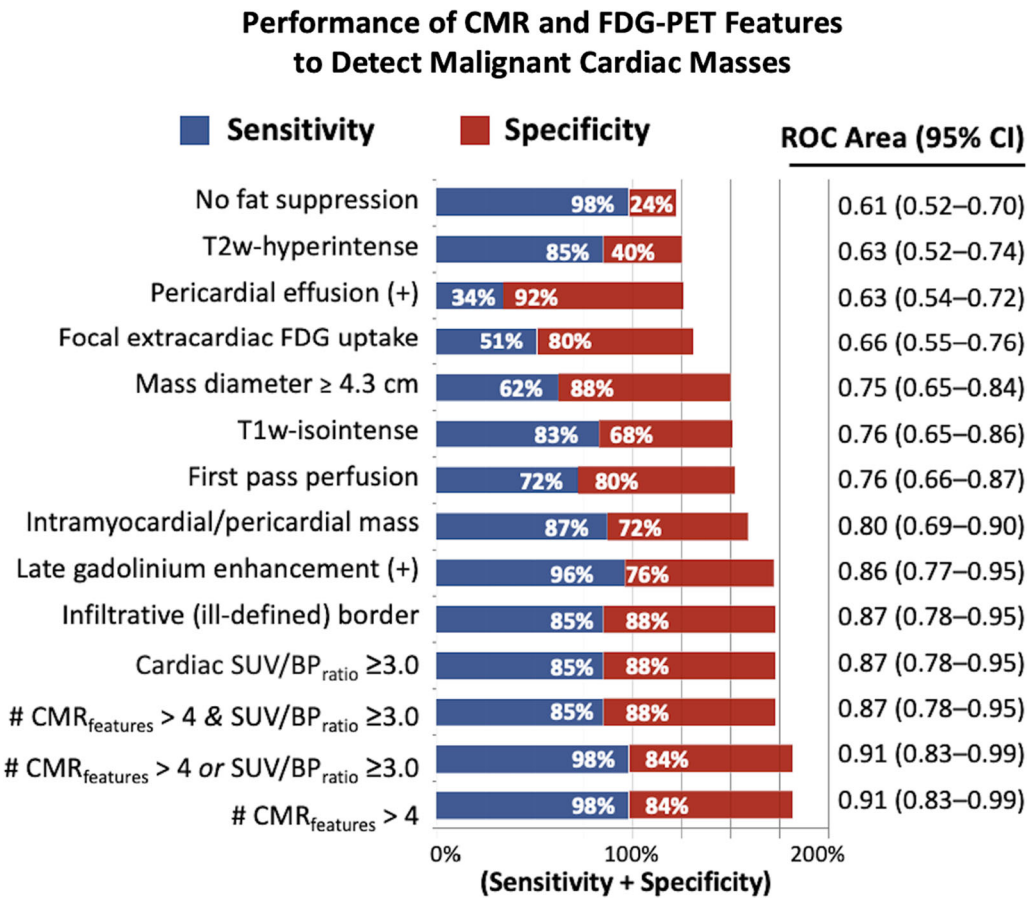

Figure 4. Ability of cardiac magnetic resonance (CMR) and fluorodeoxyglucose-positron emission tomography (FDG-PET) to detect malignant cardiac masses. Includes all patients in the current study (N = 72 patients).

died during this period. As expected, patients with malignant masses had decreased long-term survival compared with patients with benign masses (P = .006 between two groups).

In this cohort, 15 (21%) of 72 patients underwent complete resection of the cardiac mass and 5 of the masses were benign. Twenty-eight (39%) of 72 patients had chemotherapy and 13 (18%) had radiotherapy to the primary malignant focus. As demonstrated in Table 5, mortality risk was higher among patients with an infiltrative border on CMR [hazard ratio (HR) 3.1; 95% CI 1.5-6.5; P =.002] and even higher with a focal extracardiac FDG uptake [HR 3.8; 95% CI 3.8 (1.9-7.7); P <.001]. On the other hand, combined imaging features including > 4 CMR features and cardiac SUV_{max}/blood pool ratio ≥ 3.0 were not associated with increased hazards of death (P = .09).

DISCUSSION

To our knowledge, our study provides the largest examination to date of the diagnostic performance of CMR and FDG-PET/CT with prognostic data among patients with malignant and benign cardiac masses. Important findings from this analysis are (1) both CMR and FDG-PET/CT have a high accuracy in differentiating malignant tumors from benign masses, (2) more than 4 CMR features of malignancy or FDG-PET/CT SUV_{max}/blood pool ratio ≥ 3.0 have a high sensitivity (95% and 85%, respectively) and specificity (84% and 88%, respectively) to detect malignancy; and (3) an infiltrative border on CMR and focal extracardiac FDG uptake on FDG-PET/CT studies are associated with the worst prognosis (P = .002 and P < .001, respectively).

CMR imaging features of cardiac masses in our study were similar to those used in previous studies to identify malignancy.[2,8,12–14] Certain sequences alone can help to diagnose some benign cardiac masses; for

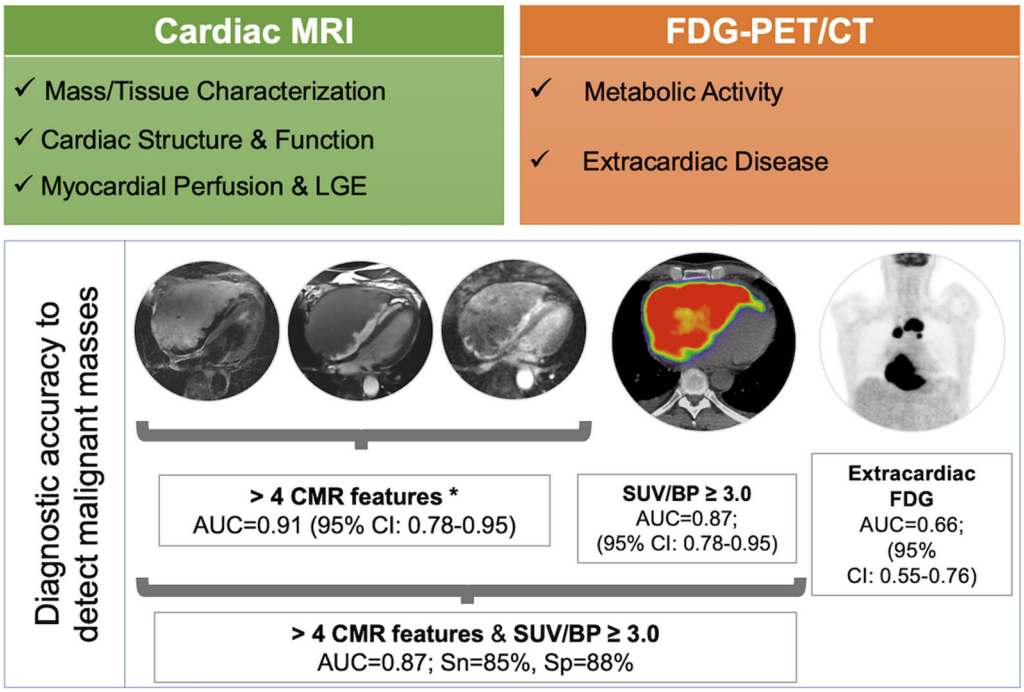

Figure 5. Complementary role of CMR and FDG-PET/CT in evaluating cardiac masses.

example, fat-suppressed images help to diagnose LHIS or lipoma, and thrombus can be identified with a long inversion time ("long TI") LGE sequence. Also, the anatomy or the shape of the cardiac masses can guide the differential diagnosis. Malignant masses typically have an infiltrative pattern with irregular or ill-defined borders, as shown previously.[11,15,16] Among the CMR features used in our study, an infiltrative appearance had the greatest combination of sensitivity (85%) and specificity (88%) to predict malignancy (AUC 0.87; 95% CI 0.78-0.95). The size of the tumor is another imaging feature to consider, and malignant cardiac tumors were often larger compared with benign masses in this cohort. Although previous studies have demonstrated that the size of the cardiac tumor is neither specific nor sensitive for predicting malignancy,[11,17] recent findings by Kassi et al. found results similar to those in our study.[12] Our study additionally finds that postcontrast sequences in all malignant tumors, including first-pass perfusion (FPP) and LGE, demonstrated mass avid enhancement consistent with previous literature.[2,8] Only 4 benign cardiac masses in our cohort showed avid FPP and LGE, including paragangliomas (N = 3) and fibroadipose tissue (N = 1). Per the World Health Organization tumor classification, paragangliomas can be either benign or malignant, and they are considered malignant when there is a metastatic focus.[18] In our study, benign (N = 3) and malignant (N = 3) cardiac paragangliomas had similar CMR imaging features. Overall, no single CMR imaging characteristic is sufficient to differentiate benign masses from malignant tumors.[2]

FDG-PET/CT data in evaluating cardiac masses and differentiating malignant from benign masses is limited.[11,19] In our study, malignant tumors demonstrated moderate-to-high FDG uptake with a median $SUV_{max/}$-blood pool ratio of 5.6 compared with 1.1 in benign masses. Optimal cardiac mass SUV_{max}/blood pool ratio to detect malignancy was ≥ 3.0, which provided the greatest combination of sensitivity (85%) and specificity (88%) to predict malignancy. Similar studies by Rahbar et al.[9] and Nensa et al.[10] suggest an absolute value of SUV_{max} of 3.5 to detect malignant tumors, with a high sensitivity (100%) and specificity (86% and 92%, respectively). Recently, a study by D'Angelo et al demonstrated SUVmax value of 4.9 to differentiate benign vs malignant masses, which is similar to our findings.[9] By pooled ROC analysis of 116 patients from studies by Nensa et al [19] and Rahbar et al.,[11] SUV_{max} ≥ 5.3 in cardiac mass demonstrated sensitivity (87%) and specificity (91%) to detect malignancy, which was similar in our cohort when absolute SUV_{max} value was used in the analysis.

Although, combining FDG-PET/CT and CMR did not increase diagnostic performance in diagnosing malignant cases, select challenging cases can benefit

Table 5. Hazard ratio for primary outcome (all-cause mortality)

	Unadjusted HR (95% CI)	*P* value	Adjusted HR (95% CI)[a]	*P* value
Age (per decile)	1.1 [0.9-1.2]	0.38	-	-
Male (N = 38)	1.0 [0.5-1.8]	0.89	1.0 [0.5-1.8][b]	.88
History of malignancy (N = 45)	1.6 [0.8-3.3]	0.19	1.6 [0.7-3.3][c]	.25
All Patients (N = 72)				
Benign, clinical diagnosis (N = 25)	Reference			
Malignant, clinical diagnosis (N = 47)	2.7 [1.3-5.6]	**0.01**	3.0 [1.4-6.5]	**.005**
Patients with Direct Histology (N = 56)				
Benign, direct pathology (N = 9)	Reference			
Malignant, direct pathology (N = 47)	4.2 [1.0-17.8]	0.05	3.8 [0.9-16.4]	.07
CMR Features (All Patients, N = 72)				
Infiltrative (ill-defined) border	3.1 [1.5-6.4]	**0.003**	3.1 [1.5-6.5]	**.002**
Mass diameter $\geq$ 4.3 cm	1.9 [1.0-3.6]	0.05	2.0 [1.0-3.9]	**.04**
Late gadolinium enhancement (+)	1.5 [0.7-3.0]	0.30	1.7 [0.8-3.6]	.16
Pericardial effusion (+)	1.4 [0.6-2.9]	0.43	1.3 [0.6-2.8]	.51
First pass perfusion (+)	1.0 [0.5-2.0]	0.93	1.2 [0.6-2.4]	.65
Intramyocardial or pericardial location	1.0 [0.5-2.0]	0.91	1.2 [0.5-2.5]	.70
Absence of fat suppression	1.0 [0.4-2.5]	0.96	1.1 [0.4-2.8]	.82
T1W isointense	0.5 [0.2-1.2]	0.13	1.1 [0.5-2.1]	.87
T2W hyperintense	0.6 [0.3-1.2]	0.12	0.4 [0.2-0.9]	**.03**
FDG-PET Features (All Patients, N = 72)				
Any focal extracardiac FDG uptake	3.9 [2.0-7.7]	**<0.001**	3.8 [1.9-7.7]	**< .001**
Cardiac $SUV_{max} \geq 5.3$	1.6 [0.8-3.2]	0.16	1.8 [0.9-3.8]	.09
Any focal cardiac FDG uptake	1.7 [0.8-3.5]	0.17	1.9 [0.9-4.1]	.11
Cardiac $SUV_{max/blood\ pool\ ratio} \geq 3.0$	1.6 [0.8-3.0]	0.19	1.9 [0.9-4.0]	.09
Combined Features (All Patients, N = 72)				
# CMR features > 4 & extracardiac FDG	3.3 [1.7-6.6]	**0.001**	3.3 [1.7-6.5]	**.001**
# CMR features > 4 & cardiac $SUV_{max} \geq 5.3$	1.6 [0.8-3.2]	0.15	1.9 [0.9-3.9]	.07
# CMR features > 4 & cardiac $SUV_{max/blood\ pool\ ratio} \geq 3.0$	1.6 [0.8-3.0]	0.19	1.9 [0.9-4.0]	.09
# CMR features > 4	1.6 [0.8-3.3]	0.19	1.9 [0.9-4.1]	.09
Management				
Complete resection (all patients, N = 15/72)	0.5 [0.2-1.1]	0.08	0.5 [0.2-1.2]	.11
Complete resection (malignant, N = 10/47)	0.3 [0.1-0.9]	**0.04**	0.3 [0.1-0.99]	**.047**
Chemotherapy (malignant, N = 28/47)	0.8 [0.4-1.7]	0.55	0.8 [0.4-1.7]	.54
Radiotherapy (malignant, N = 13/47)	1.9 [0.8-4.2]	0.13	1.8 [0.8-4.0]	.19

[a]Adjusted for age (at time of initial CMR or FDG-PET/CT), gender, and prior malignancy unless noted
[b]Adjusted for age only
[c]Adjusted for age and gender only.

from this combination. For example, FDG-PET/CT was helpful to differentiate malignant-looking benign masses on CMR, as demonstrated in the case of a fibroadipose mass, where multiple features of malignancy were noted but with minimal FDG uptake (SUV/blood pool ratio of 1.8). In our study, two cases of LHIS had focal FDG uptake, as described previously, attributed to the presence of brown adipose tissue[20] or inflammation.[21] These two LHIS cases and a fibroadipose mass case demonstrate discrepancies between CMR and FDG-PET/CT imaging features to distinguish malignant vs benign masses. On the other hand, all malignant cardiac masses demonstrated concordance between CMR and FDG-PET/CT features. Out of 47 patients with malignant cardiac mass, 46 showed more than 4 CMR features of malignancy and a high mean SUVmax of 9.6 (IQR 6.5, 13.7). One patient with squamous cell carcinoma metastasis to the heart demonstrated extensive necrosis/thrombus on histopathology, but had imaging features suggestive of a benign mass on CMR and FDG-PET/CT. As expected, it is challenging to detect "malignant cells" with any current imaging modalities. Similarly, most of the benign masses demonstrated concordance between CMR and FDG-PET/CT imaging features. Three benign paragangliomas had imaging features of malignancy both on CMR and FDG-PET/CT, but as mentioned above, paragangliomas could be either benign or malignant, and the presence of metastasis is required to diagnose malignant ones.

Although patients with malignant tumors had substantially worse long-term survival compared with patients with benign masses, overall, our cohort of patients with cardiac masses had poor long-term survival. This could be explained by the fact that more than half of the patients with benign cardiac masses (56%) had a prior history of malignancy.

Limitations

There are several limitations to this study. Our cohort consists of a single-center experience in a tertiary care referral academic center and thus there remains the potential for selection bias and a higher proportion of malignant cases relative to the general population. While our cohort includes a relatively small sample size, the current study represents the largest examination to date of cardiac mass patients with both FDG-PET/CT and CMR. Our study was retrospective in nature, and although imaging protocols were consistent throughout the study, a small number of cases omit FPP and LGE sequences. Furthermore, most patients did not have T1 or T2 mapping sequences and thus mapping relaxometry was not included in our analysis. Lastly, while FDG-PET/CT studies were performed uniformly, the absence of a standardized high-fat, low-carbohydrate diet for myocardial suppression may affect the accuracy of FDG-PET/CT findings.

CONCLUSION

Both CMR and FDG-PET/CT imaging features have high accuracy to differentiate benign and malignant masses. While combining these techniques did not increase the diagnostic accuracy for detecting malignant cardiac tumors, there was complementary diagnostic value in select cases. Moreover, while CMR was helpful in delineating the morphology of cardiac masses, providing information regarding cardiac function, as well as determining the involvement of both cardiac and non-cardiac structures, FDG-PET/CT was helpful in assessing the metabolic activity of the cardiac mass and identifying distant metastatic foci.

NEW KNOWLEDGE GAINED

1. Both CMR and FDG-PET/CT imaging features have high accuracy in differentiating benign and malignant masses, and combining these techniques did not increase the diagnostic accuracy for detecting malignant cardiac tumors; however, there is complementary value in select cases.
2. CMR imaging features (> 4 features) demonstrate a higher sensitivity (98%), and focal FDG uptake (SUV_{max}/blood pool ≥ 3.0) shows high specificity (84%) in differentiating benign vs malignant masses.
3. Combining multiple CMR imaging features and high FDG uptake (SUV_{max}/blood pool ≥ 3.0) yielded a sensitivity of 85% and specificity of 88% to diagnose malignant masses.

Disclosures

No potential conflicts of interest relevant to this article exist. Marcelo F. DiCarli, MD: received investigator-initiated institutional grants from Gilead Sciences and Spectrum Dynamics and consulting fees from Bayer and Janssen.

References

1. Butany J, Nair V, Naseemuddin A, Nair GM, Catton C, Yau T. Cardiac tumours: Diagnosis and management. Lancet Oncol 2005;6:219-28. https://doi.org/10.1016/S1470-2045(05)70093-0
2. Mousavi N, Cheezum MK, Aghayev A, Padera R, Vita T, Steigner M et al. Assessment of cardiac masses by cardiac magnetic resonance imaging: Histological correlation and clinical outcomes. J Am Heart Assoc 2019;8:e007829. https://doi.org/10.1161/JAHA.117.007829

3. Weinsaft JW, Kim HW, Shah DJ, Klem I, Crowley AL, Brosnan R et al. Detection of left ventricular thrombus by delayed-enhancement cardiovascular magnetic resonance prevalence and markers in patients with systolic dysfunction. J Am Coll Cardiol 2008;52:148–157. https://doi.org/10.1016/j.jacc.2008.03.041
4. Burke ARV Tumors of the heart and great vessels: Atlas of tumor pathology, 3rd edn1996; Armed Forces Institute of Pathology, Washington
5. Abraham KP, Reddy V, Gattuso P. Neoplasms metastatic to the heart: Review of 3314 consecutive autopsies. Am J Cardiovasc Pathol 1990;3:195-98
6. Kassop D, Donovan MS, Cheezum MK, Nguyen BT, Gambill NB, Blankstein R, Villines TC. Cardiac masses on cardiac CT: A review. Curr Cardiovasc Imaging Rep 2014;7:9281. https://doi.org/10.1007/s12410-014-9281-1
7. Kirkpatrick JN, Wong T, Bednarz JE, Spencer KT, Sugeng L, Ward RP et al. Differential diagnosis of cardiac masses using contrast echocardiographic perfusion imaging. J Am Coll Cardiol 2004;43:1412-19. https://doi.org/10.1016/j.jacc.2003.09.065
8. Pazos-Lopez P, Pozo E, Siqueira ME, Garcia-Lunar I, Cham M, Jacobi A et al. Value of CMR for the differential diagnosis of cardiac masses. JACC Cardiovasc Imaging 2014;7:896-05. https://doi.org/10.1016/j.jcmg.2014.05.009
9. D'Angelo EC, Paolisso P, Vitale G, Foa A, Bergamaschi L, Magnani I et al. Diagnostic accuracy of cardiac computed tomography and (18)F-fluorodeoxyglucose with positron emission tomography in cardiac masses. JACC Cardiovasc Imaging. 2020. https://doi.org/10.1016/j.jcmg.2020.03.021
10. Qin C, Shao F, Hu F, Song W, Song Y, Guo J, Lan X. (18)F-FDG PET/CT in diagnostic and prognostic evaluation of patients with cardiac masses: A retrospective study. Eur J Nucl Med Mol Imaging. 2019. https://doi.org/10.1007/s00259-019-04632-w
11. Rahbar K, Seifarth H, Schafers M, Stegger L, Hoffmeier A, Spieker T et al. Differentiation of malignant and benign cardiac tumors using 18F-FDG PET/CT. J Nucl Med 2012;53:856-63. https://doi.org/10.2967/jnumed.111.095364
12. Kassi M, Polsani V, Schutt RC, Wong S, Nabi F, Reardon MJ, Shah D. Differentiating benign from malignant cardiac tumors with cardiac magnetic resonance imaging. J Thorac Cardiovasc Surg. 2018. https://doi.org/10.1016/j.jtcvs.2018.09.057
13. Zhu D, Yin S, Cheng W, Luo Y, Yang D, Lin K et al. Cardiac MRI-based multi-modality imaging in clinical decision-making: Preliminary assessment of a management algorithm for patients with suspected cardiac mass. Int J Cardiol 2016;203:474-81. https://doi.org/10.1016/j.ijcard.2015.09.021
14. Fussen S, De Boeck BW, Zellweger MJ, Bremerich J, Goetschalckx K, Zuber M, Buser PT. Cardiovascular magnetic resonance imaging for diagnosis and clinical management of suspected cardiac masses and tumours. Eur Heart J 2011;32:1551-60. https://doi.org/10.1093/eurheartj/ehr104
15. Araoz PA, Eklund HE, Welch TJ, Breen JF. CT and MR imaging of primary cardiac malignancies. Radiographics 1999;19:1421-34. https://doi.org/10.1148/radiographics.19.6.g99no031421
16. Araoz PA, Mulvagh SL, Tazelaar HD, Julsrud PR, Breen JF. CT and MR imaging of benign primary cardiac neoplasms with echocardiographic correlation. Radiographics 2000;20:1303-19. https://doi.org/10.1148/radiographics.20.5.g00se121303
17. Hoffmann U, Globits S, Schima W, Loewe C, Puig S, Oberhuber G, Frank H. Usefulness of magnetic resonance imaging of cardiac and paracardiac masses. Am J Cardiol 2003;92:890-95. https://doi.org/10.1016/s0002-9149(03)00911-1
18. DeLellis RA, Lloyd RV, Heitz PU, Eng C. Pathology and genetics of tumours of endocrine organs. IARC, London; 2004
19. Nensa F, Tezgah E, Poeppel TD, Jensen CJ, Schelhorn J, Kohler J et al. Integrated 18F-FDG PET/MR imaging in the assessment of cardiac masses: A pilot study. J Nucl Med 2015;56:255-60. https://doi.org/10.2967/jnumed.114.147744
20. Fan CM, Fischman AJ, Kwek BH, Abbara S, Aquino SL. Lipomatous hypertrophy of the interatrial septum: Increased uptake on FDG PET. AJR Am J Roentgenol 2005;184:339-42. https://doi.org/10.2214/ajr.184.1.01840339
21. Zukotynski KA, Israel DA, Kim CK. FDG uptake in lipomatous hypertrophy of the interatrial septum is not likely related to brown adipose tissue. Clin Nucl Med 2011;36:767-69. https://doi.org/10.1097/RLU.0b013e318219b353